Structural Characterization and Cardioprotective Effect of Water-Soluble Polysaccharides Extracted from Clematis flammula

Intissar Baaziz, Lakhdar Ghazouani, Ilhem Rjeibi, Anouar Feriani, Kais Mnafgui, Afoua Mufti, Mounir Traikia, Didier Le Cerf, Philippe Michaud, Guillaume Pierre, et al.

applied sciences

MDPI

Article

Structural Characterization and Cardioprotective Effect of Water-Soluble Polysaccharides Extracted from *Clematis flammula*

Intissar Baaziz [1], Lakhdar Ghazouani [1], Ilhem Rjeibi [1], Anouar Feriani [1], Kais Mnafgui [2], Afoua Mufti [1], Mounir Traikia [3], Didier Le Cerf [4], Philippe Michaud [5], Guillaume Pierre [5,*] and Slim Cherif [6]

1 Laboratory of Biotechnologies and Biomonitoring of the Environment and Oasis Ecosystems (LBBEEO), Faculty of Sciences of Gafsa, Gafsa 2112, Tunisia
2 Laboratory of Plant Biotechnology, Faculty of Science, University of Sfax, B.P. 1171, Sfax 3000, Tunisia
3 SIGMA Clermont, Institut de Chimie de Clermont-Ferrand, Université Clermont Auvergne, CNRS, 63000 Clermont-Ferrand, France
4 Normandie Université, UNIROUEN, INSA Rouen, CNRS, PBS, 76000 Rouen, France
5 Clermont Auvergne INP, CNRS, Institut Pascal, Université Clermont Auvergne, 63000 Clermont–Ferrand, France
6 Laboratory of Biochemistry and Enzymatic Engineering of Lipases, National Engineering Scholl of Sfax, University of Sfax, Sfax 3038, Tunisia
* Correspondence: guillaume.pierre@uca.fr; Tel.: +33-(0)-473-407-422

Abstract: *Clematis flammula* is widely used for its pharmacological properties in Tunisia. This work aimed to explore, in a rat model, the cardiopreventive capacity of polysaccharides extracted from *C. flammula* (CFPS) after a myocardial injury caused by isoproterenol. Structural analyses suggested that the average molecular weight of CFPS was 1.82 × 10^5 g/mol, being mainly composed of glucuronide (41.53%), galacturonic acid (19.06%), arabinose (16.10%), galactose (6.15%), glucose (5.49%), and rhamnose (3.55%). Fourier transform–infrared spectroscopy and nuclear magnetic resonance spectroscopy experiments showed that CFPS was rich with carbohydrates containing pectic materials with glycosidic bonds. In addition, results show that pretreatment with CFPS (150 mg/kg) could improve the electrocardiogram pattern by decreasing the elevated ST segment and ameliorating the relative heart weights and the biochemical profile content (creatine phosphokinase-MB, lactate dehydrogenase, and cardiac troponin I). Furthermore, pretreatment with CFPS reduced the amount of malondialdehyde and restored the genotoxicity induced by isoproterenol. The histopathological study revealed that CFPS pretreatment diminished the level of cardiac tissue injury. Based on these data, CFPS presents a broad biological effect as a cardioprotective and can be used for the exploration of novel natural products for the treatment of cardiac disease.

Keywords: *Clematis flammula*; polysaccharides; cardioprotective; genotoxicity; myocardial injury

Citation: Baaziz, I.; Ghazouani, L.; Rjeibi, I.; Feriani, A.; Mnafgui, K.; Mufti, A.; Traikia, M.; Le Cerf, D.; Michaud, P.; Pierre, G.; et al. Structural Characterization and Cardioprotective Effect of Water-Soluble Polysaccharides Extracted from *Clematis flammula*. *Appl. Sci.* **2022**, *12*, 10818. https://doi.org/10.3390/app122110818

Academic Editor: Burkhard Poeggeler

Received: 12 September 2022
Accepted: 19 October 2022
Published: 25 October 2022

1. Introduction

Heart attacks represent a major form of coronary heart alteration. They occur as the result of unbalanced cardiac demand and coronary artery supply of nutrients and oxygen [1,2]. This imbalance leads to degeneration of cardiomyocytes and thereafter to cardiac ischemia [3], causing damage to myocardium tissue associated with irreversible heart cells' death or injury [4]. Even though clinical care and therapeutic modalities have improved in cardiovascular disease treatment, acute ischemic heart remains the leading cause of death in the world with seven million individual deaths [5].

High-acute-dose administration of a synthetic catecholamine, "Isoproterenol" (ISO), was used experimentally in animals to produce deleterious effects on the heart function, such as myocardium alteration, fibrosis, apoptosis, hypertrophy, necrosis, and inflammatory cell infiltration [6,7]. The morphological and pathophysiological aberrations taking place

in the infarcted rat model were like those seen in myocardial injury (MI) patients [8]. This experiment was used to investigate the cardioprotective capacity of several molecules against human MI [9].

The application of medicinal plants has long been used in different countries in Africa [10]. Vegetable and fruit intake can thus be used to reduce the chance of developing cardiovascular pathology [11]. Various herbal medicines have been revealed to have major cardioprotective properties [12] and a powerful neutralization capacity against free radicals. [13,14]. Polysaccharides, with diverse class of macromolecules, are an important class of biopolymers. Recently, the pharmacological role of poly- and oligosaccharides as well as enriched fractions has been deeply studied [15]. Plant polysaccharides are primarily of interest due to their numerous biological activities, ranging from antioxidant, anti-inflammatory, and anticancer properties to antiviral and anti-hyperlipidemic activities [16].

Clematis species are widely distributed in the Northern Hemisphere, which explains their widespread use in traditional medicines. In Europe and Eastern Asia, people use the aerial parts to treat eye infections, bone illnesses, gout, fever, and chronic skin disorders [17,18]. Chinese people use *Clematis* species against wind-cold rheumatism [19]. Furthermore, it has been reported that some species, such as *C. flammula*, showed antifungal activity [20], cytotoxic activity, an anti-inflammatory effect and also antioxidant potential to deal with potential arthritis, superficial burns, and cancer [21]. It has been reported that polysaccharides from *C. huchouensis* Tamura (acidic proteoglycan) possess important scavenger activity [22]. A flavonoid extracted from *C. tangutica* ameliorates myocardial alteration [23]. Other glycosides of *C. lasiandra* Maxim exhibited significant protection against tumor cell lines [24]. In Tunisia, the ethnopharmacological data obtained from herbalists highlighted that *C. flammula* (Ranunculaceae) has been used traditionally to treat skin diseases [25].

The goal of this work was to study the preventive capacity of an enriched polysaccharide fraction extracted from the aerial part of *Clematis flammula* (CFPS) against isoproterenol-induced MI in a rat model (male Wistar rats). Thus, electrocardiogram (ECG) patterns, heart oxidative stress, biochemical markers, apoptosis tests, and the myocardial pathology were explored. Furthermore, the CFPS fraction was structurally characterized by colorimetric assays, high-pressure size-exclusion chromatography (HPSEC), size-exclusion chromatography coupled with multi-angle laser-light scattering (SEC-MALS), gas chromatography coupled to mass spectrometry (GC/MS), Fourier transform–infrared spectroscopy (FT-IR), and nuclear magnetic resonance spectroscopy (NMR) experiments to partly correlate the biological functions studied in this paper with the main identified structural features.

2. Materials and Methods

2.1. Plant Material and Chemicals

The aerial parts of *Clematis flammula* were harvested in May 2019, from Sened, in the Gafsa region of south Tunisia (34°27′46″ N latitude and 9°15′51″ E longitude). The species was identified by Dr. Zouhaeir Abbes. The leaves and flowers were washed, dried, and then ground into a powder (50–200 mesh) and finally kept at room temperature until use.

2.2. Extraction and Purification of CFPS Fraction from the Aerial Part of C. Flammula

The CFPS fraction was extracted using the protocol described by Rjeibi et al. [26]. Briefly, the dried leaf and flower powder (200 g) was first depigmented and delipidated sequentially with acetone and ethanol (7:3 *v*:*v*) for 1 h at 40 °C under moderate stirring (300 rpm). The depigmented and defatted biomass was dried in an oven for 3 h at 50 °C and then extracted using hot water for 2 h at 70 °C under stirring (300 rpm). After centrifugation (3750× *g*) for 20 min using a refrigerated centrifuge (ThermoJouan GR4i, Thermo Fisher Scientific, Munich, Germany), the supernatant was precipitated overnight by adding 3 volumes of cold ethanol (96%, −20 °C) under gentle stirring (140 rpm). The crude enriched fraction in polysaccharides was then obtained through another centrifugation step (8000× *g*, 15 min, 4 °C), followed by ethanolic precipitations (three times) following

the same procedure (the conductivity was controlled). The final pellet was solubilized in ultrapure water and then lyophilized to obtain the enriched polysaccharide fraction, called CFPS.

2.3. Preliminary Study of CFPS

2.3.1. Biochemical Composition

Colorimetric assays were used to determine the biochemical composition of CFPS. Total carbohydrate contents were estimated using the phenol–sulfuric acid method [27], D-glucose being used as the standard. Neutral sugars and uronic acids were measured with the sulfuric resorcinol assay [28] and *m*-hydroxybiphenyl methods [29], using glucose and glucuronic acid as standards, respectively. Total phenolic compounds were determined using the Folin–Ciocalteu procedure, gallic acid being used as the standard [30]. The concentration in proteins was determined using the micro-Bradford assay using bovine serum albumin as the standard [31].

2.3.2. Fourier Transform–Infrared Spectroscopy (FT-IR) Analysis

The FT-IR spectrum of CFPS was determined using a VERTEX 70 FTIR instrument ATR A225 diamante (Bruker VERTEX 70, Ettlingen, Germany). Fifty scans were measured at room temperature (referenced against air) in the frequency range of 4000 to 400 cm^{-1}. The data were analyzed with OPUS 7.2 software (Bruker, Ettlingen, Germany).

2.3.3. Monosaccharide Composition Analysis with GC/MS

The analysis of the trimethylsilylated monosaccharides was carried out using gas chromatography (GC). In total, 15 mg of CFPS was solubilized in 1.5 mL of TFA (2 M) and heated for 90 min at 120 °C to release the residues. The hydrolysate was then evaporated under a nitrogen stream (60 °C). Monosaccharide derivatization was carried out following a method adapted from Pierre et al. [32,33] using BSTFA: TMCS (99:1) (2 h, 30 °C). The mixture was then dried under a nitrogen stream, and the trimethylsilyl-*O*-glycosides were resuspended into dichloromethane (10 g/L). The same procedure was repeated using standard monosaccharides (mannose: Man, glucose: Glc, arabinose: Ara, rhamnose: Rha, ribose: Rib, fucose: Fuc, xylose: Xyl, fructose: Fruc, mannuronic acid: ManA, galactose: Gal, glucuronic acid: GlcA, and galacturonic acid: GalA). Glucuronide and glucoside amounts were estimated using GlcA- and Glc-adapted standard curves. The samples were injected on a Shimadzu Nexus GC-2030 coupled to a GCMS-QP2020NX (Shimadzu, Japan), equipped with an OPTIMA-1MS Accent column (Macherey-Nagel; 30 m, 0.25 mm, 0.25 µm) from Macherey-Nagel with a hydrogen flow rate of 1.75 mL/min (7.8 psi). The initial temperature was set at 100 °C for 2.75 min, followed by a rise of 8.40 °C/min until reaching 200 °C. A second increase in temperature was set at 5.20 C/min until 215 °C was reached, and this was held for 0.95 min. The electronic impact (EI, 70 eV) ionization method was performed with the trap temperature set at 150 °C, and the target ion was fixed at 40–800 m/z. The solvent cut time was set at 5 min, the split ratio was 50: 1, and the temperature of the injector was 250 °C. The relative molar proportions were determined using area normalization. The data were analyzed using MestReNova Software 7.1.0-9185 (Mestrelab Research, Coruña, Spain).

2.3.4. Molecular Structural Characteristics

- Determination by HPLC-RID

The molecular weight of CFPS was firstly estimated by HPSEC (HPLC 1100 series, Agilent, Palo Alto, CA, USA) coupled to a refractive index detector (RIDG1362, Agilent). Two columns (TSKgel PWXL Type Guard column 5000 and 3000, Tosoh Bioscience GMBH, Stuttgart, Germany) were eluted with sodium nitrate ($NaNO_3$, 0.1 M) at 50°C and 1 mL/min, using pullulan standards as standards for calibration (from 1.3 to 800 kDa, 10 g/L). $NaNO_3$ (0.1 M) was used to solubilize CFPS (10 g/L) for 24 h at room temperature under magnetic stirring (350 rpm) before injection (20 µL). The number (M_n) and weight

(M_w) average molecular weights and the polydispersity index (Đ) were calculated with Equations (1)–(3):

$$M_n = \frac{\sum N_i M_i}{\sum N_i} \quad (1)$$

$$M_w = \frac{\sum N_i {M_i}^2}{\sum N_i M_i} \quad (2)$$

$$= \frac{M_w}{M_n} \quad (3)$$

where M_i and N_i are the molecular weight and number of moles of polymer species, respectively.

- Determination by SEC-MALS

Other molecular characteristics of the CPFS fraction were estimated in the dilute regime by HPSEC (HELEOS II, Wyatt Technology Corp) coupled to three detectors: (i) a He-Ne laser at 690 nm (HELEOS II, Wyatt Technology Corp, Santa Barbara, CA, USA); (ii) a multi-angle laser-light scattering (MALS) filled with a K5 cell (50 L); (iii) a differential refractive index (RID 10A, Shimadzu, Japan); and a viscosimeter (ViscostarII, Wyatt Technology Corp., Goleta, CA, USA). Two columns (OHPAK SB-G guard column, OHPAKSB806 and 804 HQ columns (Shodex)) were eluted with $LiNO_3$ 0.1 M at 0.5 mL/min. CFPS was solubilized at 1 g/L in 0.1 M $LiNO_3$ solution for 72 h under stirring (200 rpm) at room temperature, filtered (0.45 µm), and then injected through a 100 µL full loop.

2.3.5. NMR Spectrometric Analysis

For NMR analysis, CFPS was dissolved at 50 g/L in D_2O and freeze-dried to substitute exchangeable proton with deuterium (3 times). NMR spectra were obtained at 353 K on a Bruker AVANCE III HD 500 MHz spectrometer equipped with a Bruker 5 mm inverse probe TXI ($^1H/^{13}C/^{15}N$) with a z-gradient coil probe. The ^1H NMR spectrum was acquired using a ZG sequence. A total of 128 scans were collected with the following parameters: (i) 90 impulsion time of 9.7 µs at a power of 14 W, (ii) 4 s relaxation time, (iii) an acquisition of 3.3 s, (iv) a spectral window of 20 ppm, and (v) 65 K data points zero-filled to 131 K before Fourier transformation with 0.3 Hz line broadening.

2.4. In Vivo Study

2.4.1. Animals

The experimental protocols that were used in this study were approved by the Ethical Committee for the Care and Use of Laboratory Animals at the University of Gafsa (reference no: FSG-AE-20-23). The whole experiment was carried out using 32 male Wistar rats (sixty days old and weighing 280–290 g). The animals were acquired from the Central Pharmacy of Tunisia. Rats were kept in standard cages for a one-week acclimatization period in a hygienic and clean environment at around 20 °C and 60 ± 5% humidity with an alternate 12 h cycle of dark and light. The animals had free access to water and a standard diet.

2.4.2. Experimental Induction in Rats

Isoproterenol (ISO) was dissolved in 2 mL of physiological saline and injected into rats subcutaneously (85 mg/kg body weight/day) on the 14th and 15th days to induce experimental MI [34].

2.4.3. Acute Toxicity Study

The acute toxicity assays were conducted by administering CFPS extracts at the following doses: 5, 25, 50, 75, and 100 mg/kg body weight. Then, the general behavior and the number of deaths were monitored from 24 h following administration of the extracts onwards, and it was continued within 14 days of the administration of the substances. No change, clinical sign of toxicity, or mortality was observed in animals up to a dose of 100 mg/kg bw until the end of the experiment.

2.4.4. Experimental Protocols

After the acclimatization, 32 male Wistar rats were randomly allocated into 4 groups of 8 rats each:

- Group I: vehicle control rats, received standard laboratory diet and saline water ad libitum for 15 days.
- Group II: ISO-treated rats, received saline water for 15 days, and subcutaneously injected with ISO (85 mg/kg body weight) on the 14th day and 24 h later.
- Group III (ISO + CFPS): rats were given CFPS at a dose of 100 mg/kg daily for 15 days by gastric gavage and subcutaneously received ISO (85 mg/kg body weight) for two consecutive days (14th and 15th days)
- Group IV (ISO + Pid): Rats were treated with pidogrel (Pid) 150 µg/kg body weight orally) for 15 days and were subcutaneously injected with ISO (85 mg/kg body weight) on the 14th and 15th day.

2.4.5. Electrocardiography

Twenty-four hours later, after the second dose of ISO, touch electrodes were inserted under the skin of animals included in all the groups under light ether anesthesia with ketamine hydrochloride (80 mg/kg, i.p.) in lead II position. CG) patterns were monitored by using a veterinary electrocardiograph (ECG VET 110, Biocare, China).

2.4.6. Biochemical Assay

After recording the ECG of anesthetized rats, the animals were anesthetized with ketamine hydrochloride (100 mg/Kg bw) intraperitoneally and decapitated.

The plasma was separated by centrifugation (3500 rpm; 10 min; 4 °C) and directly used for the analysis of plasmatic creatine phosphokinase-MB (CK-MB) and lactate dehydrogenase (LDH). Plasma activities of CK-MB and LDH were expressed as units per liter. The amount of plasma cardiac troponin-I ($ng.mL^{-1}$) was measured using a standard kit by electrochemiluminescence immunoassay (Roche Diagnostics, Switzerland, Ref, 07007302 119). The lipid profile, including total cholesterol, triglycerides, and LDL cholesterol, was determined according to routine procedures using commercial reagent kits purchased from Biolabo (France).

2.4.7. Determination of Lipid Peroxidation

The level of lipid peroxidation in the heart of all the groups of animals was determined by measuring the concentrations in malondialdehyde (MDA). For this purpose, a thiobarbituric acid reaction was monitored at λ = 532 nm (Shimadzu UV-1800, Shimadzu, Canby, OR, USA) as described previously by Ohkawa et al. [35], and the results are expressed as nmol concentration of MDA per mg of proteins.

2.4.8. DNA Fragmentation Assay

DNA in the targeted tissue of the studied animals was extracted using the phenol–chloroform–isoamyl alcohol method [36]. The DNA was extracted after adding a volume of phenol–chloroform–isoamyl alcohol (25:24:1) (v:v:v). In total, 5 µL of RNase A (Sigma-Aldrich, St. Louis, MO, USA) at 20 mg/mL was added and then incubated for 15 min to degrade all cellular RNAs.

Qualitative damage of genomic DNA was carried out by electrophoresis on 0.8% agarose–ethidium bromide gel staining. Thirty-one intact and fragmented DNA fractions were visualized under UV light [37].

2.4.9. Measurement of Myocardial Infarction Area

The myocardial infarct size was determined using the triphenyl tetrazolium chloride (TTC) test according to the method described by Khalil et al. [38]. Briefly, sections of the removed heart tissue were stained with 1% 2, 3, 5-TTC dissolved in PBS at 37 °C for 20 min. A light

microscope was used to evaluate these sections, and infarct size was calculated by dividing the infarct ischemic region, which appeared as white, by the total area (white and red).

2.4.10. Histopathological Studies

After sacrificing the animals, the heart tissues of each rat were immediately dissected and fixed in 10% buffered formalin solution. The fixed tissues of liver were inserted in paraffin, cut into multiple sections of 5 µm, and then stained with hematoxylin and eosin (H&E) to evaluate myocardial necrosis, edema, and inflammatory cell infiltration. Various photos of the tissues were obtained by a light microscope up to and at 200× *g* magnification (Olympus CX41 microscope (Tokyo, Japan).

2.5. Statistical Tests

The data are expressed as the mean ± standard deviation (SD). A one-way ANOVA with a Tukey post hoc test was used along with the Graph-Prism 7.01 software (GraphPad, San Diego, CA, USA). Post hoc tests were used as a follow-up to the ANOVA to determine which pairwise comparison of means contributes to the overall significant difference. Data were considered statistically significant at $p < 0.05$.

3. Results

3.1. Chemical Composition

The physicochemical parameters of CFPS are shown in Table 1. The results show that the extracted yield was 6.5%. Following the phenol–sulfuric acid test, carbohydrates were determined to be the most important content in the crude polysaccharides (34.5%). The uronic acid and neutral sugar contents were about 17.81 and 16.11%, respectively. Furthermore, the results also reveal that CFPS contained small amounts of total phenol (1.6%). Meanwhile, the protein content of CFPS was about 2.5%, which indicated the good purity of the extracted polysaccharides.

Table 1. Global composition of CFPS fraction extracted from *Clematis flammula*.

Extraction Yield (%, *w*/*w*)	Total Carbohydrates (%, *w*/*w*)	Uronic Acids (%, *w*/*w*)	Neutral Sugars (%, *w*/*w*)	Proteins (%, *w*/*w*)	Phenolic Compounds (%, *w*/*w*)	(NaCl) eq. (%)	Conductivity (µs/cm)
6.5	34.5 [a] ± 0.35 38.1 [b] ± 1.1	17.81 ± 0.25	16.11 ± 0.12	2.5 ± 0.45	1.6 ± 0.12	8.26	110

Values are means ± SD (n = 3) as measured using a [a] colorimetric assay and [b] quantified by GC/MS-EI.

3.2. Preliminary Structural Features of CFPS

3.2.1. FT-IR Spectra

FT-IR was used to pre-identify (footprint) functional groups of CFPS (Figure 1). CFPS presented a typical polysaccharide spectrum [39,40] with a strong and broad absorption bond observed at 3273 cm^{-1} that was assigned to O-H stretching vibrations of water and carbohydrates. The peak at 2361 cm^{-1} was due to the lack of CO_2/H_2O normalization during the data treatment. The two peaks at 1596 cm^{-1} and 1402 cm^{-1} were attributed to carboxylate groups of uronic acid residues but could also correspond to the overlap of glucuronide/glucoside or methyl–sugar structures. The absorption band at 1095 cm^{-1} (from 1000 cm^{-1} to 1200 cm^{-1}) corresponded to the stretching vibration of polysaccharides. The bands around 885 cm^{-1} could be due to β-linked polysaccharides. Note that some proteins (traces) could also be detected owing to the band close to 1321 cm^{-1}.

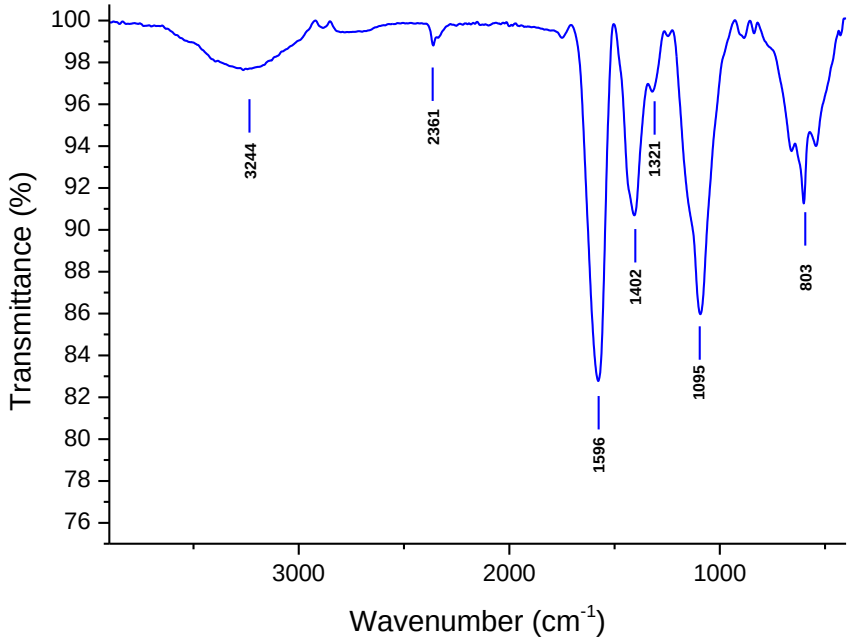

Figure 1. ATR-FTIR spectrum of CFPS.

3.2.2. Monosaccharide Composition

The monosaccharide content of CFPS was explored using GC/MS (Table 2). CFPS was rich in glucuronide (41.53%), Ara (16.10%), and Glc (5.49%). Minor levels of galacturonic acid (19.06%), galactose (6.15%), and rhamnose (3.55%) were seen as a result of the presence of pectic polymers [41]. These results suggest that CPFS is a fraction enriched in carbohydrates containing pectic materials (GalA, Rha, and Ara) as well as glucuronides and glycosides.

Table 2. Characterization of CFPS fraction extracted from *Clematis flammula*.

M_w [a] (g/mol)	M_n [b] (g/mol)	Đ [c]	Rh [d] (nm)	[η] [e] (mL/g)	Monosaccharides [f] (mol%)							
					Ara	Rha	Gal	Glc	GalA	Glucuronide	Glucoside	Me-Hexp
1.82×10^5	4.68×10^4	3.89	21	165	16.1	3.55	6.15	5.49	19.1	41.5	5.08	3.02

Analyses were run in duplicate, and the relative standard deviations were less than 5%. [a] Mw: weight-average molecular weight was measured by HPSEC. [b] Mn: number-average molecular weight was measured by HPSEC. [c] Đ: polydispersity index Mw/Mn. [d] Rh: hydration radius was determined by SEC-MALLS. [e] [η]: intrinsic viscosity was determined by SEC-MALLS. [f] Monosaccharide composition was determined by GC/MS-EI. Glc: glucose, GalA: galacturonic acid, Gal: galactose, Ara: arabinose, Rha: rhamnose, Me-Hexp: methyl-hexopyranose.

3.2.3. Macromolecular Characteristics of CFPS

The CPFS fraction was analyzed using both HPSEC-RID and SEC-MALS. The Mw and Mn of CFPS were 1.82×10^5 and 4.68×10^4 g.mol^{-1}, respectively, with a significant polydispersity index value (3.89), highlighting the partial heterogeneity of CFPS (Table 2), which was consistent with the presence of pectic materials, glucuronides, and glycosides. These values were in the same range as those found for water-soluble polysaccharides extracted from Ranunculaceae such as *Aconitum coreanum* (340 kDa) [42]. The intrinsic viscosity [η] and hydrodynamic radius (Rh) values, which are used for understanding the rheological behavior of hydrocolloids in solutions, were 165 mL/g and 21 nm, respectively, for CFPS. As described in the literature, these values depend on the molecular weight and the conformation of polymer chains in solvents [43]. The critical concentration C*, defined by 1–4/[η], can be theoretically estimated as ranging from 0.61% to 2.42% (w/v).

3.2.4. NMR Investigation

The polysaccharides extracted from *C. flammula* were qualitatively analyzed using ^{1}H NMR spectroscopy (Figure 2). In combination with the constituent monosaccharides of CFPS, the weak signal at 1.11 ppm was assigned to the methyl groups of rhamnose. The set of signals at (3.41–4.31 ppm) was assigned to the characteristic resonances of the proton ring (H2–H5) [44]. Furthermore, the presence of several anomeric signals in the region between 4.45 and 4.65 ppm indicates the presence of terminal galactose [45]. These indicate that the fraction contained galactan side chains and agreed with the sugar composition. Other signals observed at 5.12 ppm, 4.05 ppm, 3.88 ppm, and 4.02 ppm were clearly assigned to H-1, H2, H-3, and H-4, respectively, of the terminal arabinosyl residue [46].

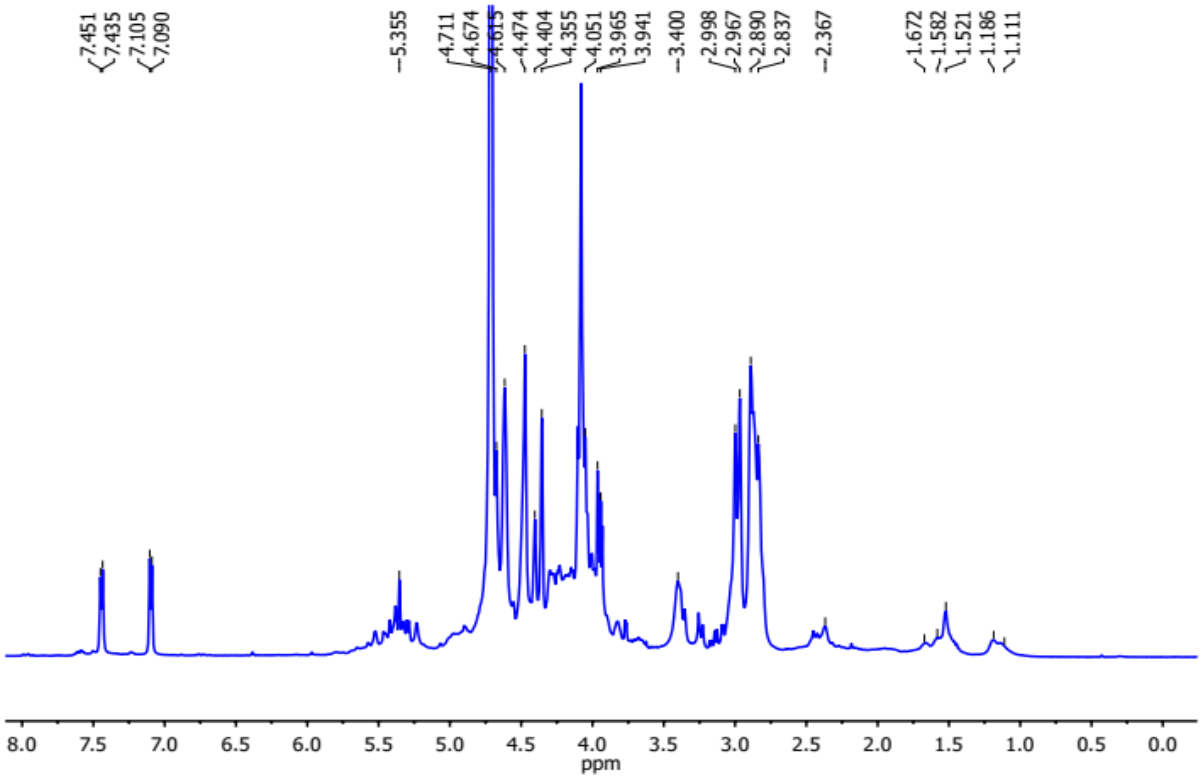

Figure 2. ^{1}H NMR spectra of CFPS from *Clematis flammula*.

3.3. In Vivo Activities

3.3.1. Heart Weight and Body Weight

The heart weight and body weight of treated rats are shown in Table 3. The rats intoxicated with isoproterenol revealed an obvious elevation in the heart weight ($p < 0.01$) and an insignificant change in body weight, as compared to controls. Pretreatment with pidogrel or CFPS showed a remarkable reduction in relative heart weights by 12% and 8% ($p < 0.05$), respectively, compared to the ISO-treated group. No differences were observed between the CFPS + ISO and the Pid + ISO groups ($p < 0.05$).

Table 3. Effect of CFPS fraction on body weight, heart weight, and cardiac weight index (CWI) of control and experimental groups of rats.

	Control	ISO	Pid + ISO	CFPS + ISO
Body weight (g)	293.5 ± 2.31	294.4 ± 2.55	295.3 ± 1.76	294.6 ± 2.79
Heart weight (g)	0.75 ± 0.01	1. 32 ± 0.08 *	1.02 ± 0.09 ¥	1.01 ± 0.12 ¥
CWI	0.25 ± 0.01	0.44 ± 0.01 *	0.35 ± 0.01 ¥	0.34 ± 0.02 ¥

Values are expressed as mean ± SD of eight rats in each group. * $p < 0.05$: controls vs. ISO. ¥ $p < 0.05$: CFPS + ISO or Pid + ISO vs. ISO.

3.3.2. Effect of CFPS on ECG Findings

Figure 3 reveals that normal rats represented an ECG pattern with regular sinus rhythm. In contrast, as compared to the control group, ISO-treated rats exhibited remarkable changes in ECG pattern, as well as ST segment elevation (Supplementary Data). The combination with CFPS (100 mg/kg) attenuated ECG pattern changes and mitigated conduction abnormalities when compared to the ISO-treated rats alone, which confirmed its ameliorating role in the heart membrane.

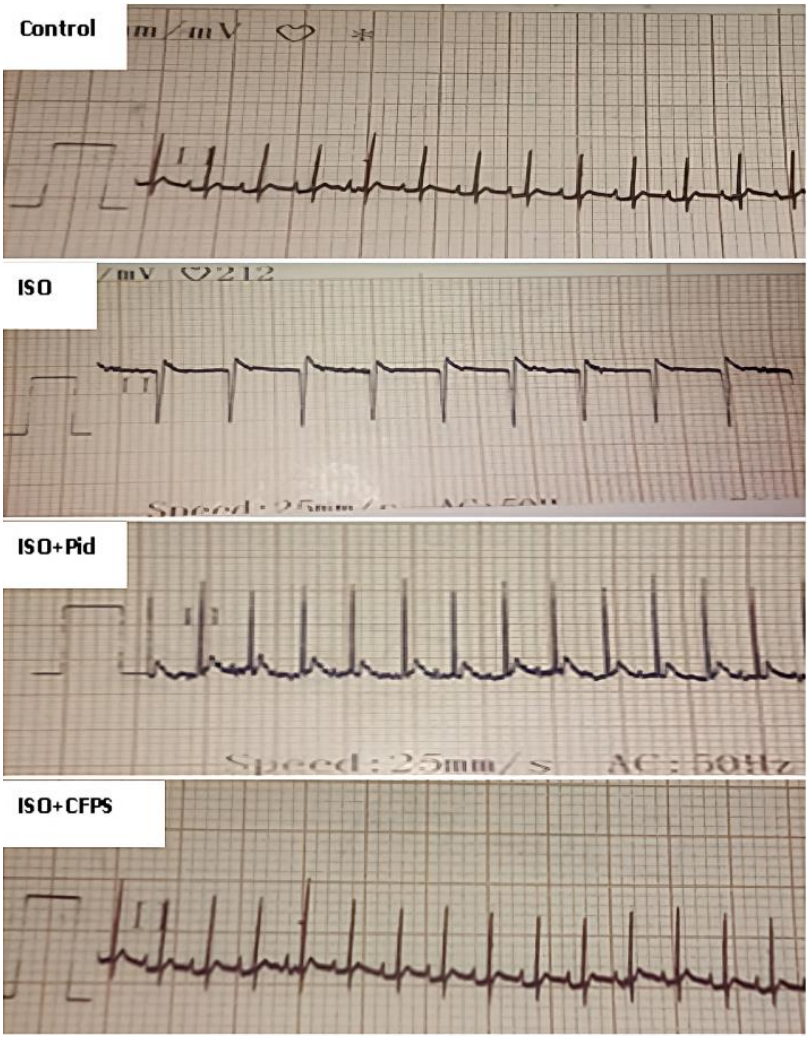

Figure 3. Effect of CFPS on electrocardiographic (ECG) pattern in treated animals. Control: recording of the control rats. ISO: recordings of the rats injected with isoproterenol (85 mg/kg). ISO + Pid: recording of rats precotreated with pidogrel (Pid) and injected with isoproterenol. Iso + CFPS: recording of rats precotreated with CFPS and injected with isoproterenol.

3.3.3. Cardiac Injury Biomarkers

The activities of cardiac marker enzymes in the plasma of experimental animals are shown in Table 4. The activity of plasmatic creatine phosphokinase-MB (CK-MB) and lactate dehydrogenase (LDH) as well as the amount of cardiac troponin I (cTn-I) were remarkably increased ($p < 0.05$) by 413%, 124%, and 187%, respectively, in the ISO-treated group as compared to normal animals. The combination with CFPS extract prevented the side effect of ISO and thereafter the levels of the biochemical markers, as compared to intoxicated animals alone. Similar results were observed for pidogrel treatment. The results also reveal that the CFPS treatment exhibited a lower protective effect than the Pid treatment against ISO administration.

Table 4. Effect of CFPS fraction on cardiac biomarkers.

	Control	ISO	ISO + Pid	Iso + CFPS
cTn-I (ng/mL)	0.44 ± 0.05	2.26 ± 0.13 *	1.32 ± 0.03 ¥	1.45 ± 0.12 ¥,β
CK-MB (U/L)	57.43 ± 1.30	128.9 ± 1.50 *	95.35 ± 1.11 ¥	102.3 ± 1.00 ¥,β
LDH (U/L)	58.03 ± 1.66	166.7 ± 1.32 *	129.9 ± 1.45 ¥	134.4 ± 0.72 ¥,β

All values are given as mean ± SD (n = 8). * $p < 0.05$: controls vs. ISO. ¥ $p < 0.05$: CFPS + ISO or Pid + ISO vs. ISO. β $p < 0.05$: CFPS + ISO vs. Pid + ISO.

3.3.4. Effect of CFPS on Fibrinogen Level

The content of fibrinogen in treated groups is shown in Figure 4. The data reveal that rats treated with ISO exhibited a significant increase of 51% in plasma fibrinogen concentration when compared to normal animals. Administration of CFPS in intoxicated rats decreased the plasma fibrinogen amount by 51% as compared to infarcted rats. Moreover, the pretreatment with pidogrel in infracted rats evidenced a nearly similar result in reducing the plasma level of fibrinogen by 55% in comparison to the ISO group.

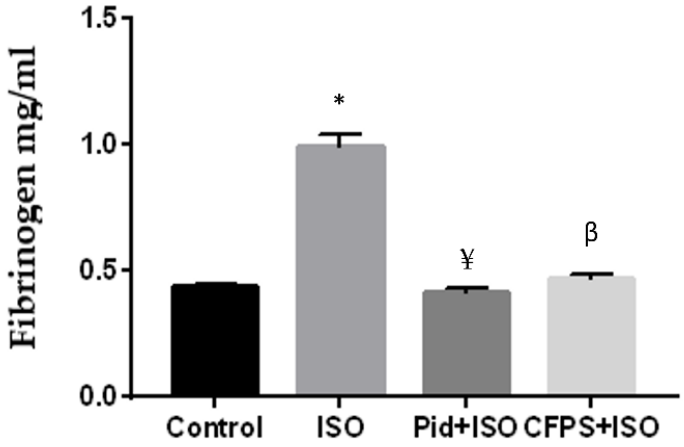

Figure 4. Plasma fibrinogen level variation in control and experimental rats. Values are given as mean ± SD for groups of 8 animals each. * $p < 0.05$: controls vs. ISO. ¥ $p < 0.05$: CFPS + ISO or Pid + ISO vs. ISO. β $p < 0.05$: CFPS + ISO vs. Pid + ISO.

3.3.5. Lipid Profile

The results show that, as compared to normal rats ($p < 0.05$), the amounts of total cholesterol, triglycerides, and LDL cholesterol were increased by 38%, 41%, and 122%, respectively, in ISO-induced myocardial infarcted animals (Table 5). It was remarkable that the pre/cotreatment with CFPS near normalized the levels of these targeted parameters in the plasma of rats treated with ISO. Significant differences in the profiles of enzymes were observed between the CFPS + ISO group and the Pid + ISO group.

Table 5. Effect of CFPS fraction on lipidic profile.

	Control	Iso	ISO + Pid	Iso + CFPS
TC (mg/dL)	86.19 ± 1.18	118.6 ± 2.11 *	93.48 ± 0.66 ¥	100.1 ± 1.26 ¥,β
TG (mg/dL)	40.26 ± 0.72	56.69 ± 1.44 *	48.58 ± 0.90 ¥	51.04 ± 0.91 ¥,β
LDL-c (mg/dL)	29.25 ± 0.63	64.99 ± 0.87 *	35.82 ± 1.04 ¥	40.76 ± 0.46 ¥,β

All values are given as mean ± SD (n = 8). * $p < 0.05$: controls vs. ISO. ¥ $p < 0.05$: CFPS + ISO or Pid + ISO vs. ISO. β $p < 0.05$: CFPS + ISO vs. Pid + ISO.

3.3.6. Effects of CFPS on the Lipid Peroxidation

The cardiac MDA level of all treated groups is illustrated in Figure 5. ISO injection induced heart oxidative stress as manifested by the increased MDA level, an indicator of

lipidic peroxidation. However, the administration of CFPS or pidogrel revealed a significant reduction in MDA levels ($p < 0.05$) when compared to isoproterenol alone. Significant differences in the profiles of enzymes were observed between the CFPS + ISO group and the Pid+ISO group.

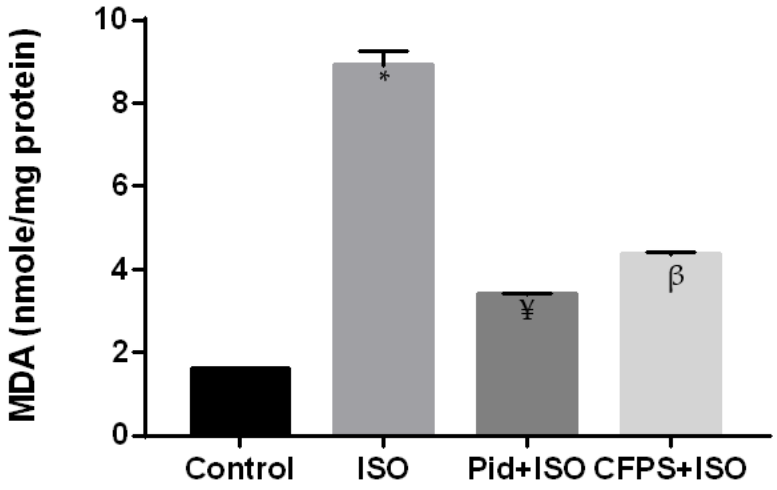

Figure 5. Effect of CFPS precotreatment on lipid peroxidation products in the heart tissues of the control and experimental groups of rats. Values are expressed as mean ± SD (n = 8). * $p < 0.05$: controls vs. ISO. ¥ $p < 0.05$: CFPS + ISO or Pid + ISO vs. ISO. β $p < 0.05$: CFPS + ISO vs. Pid + ISO.

3.3.7. DNA Fragmentation Analysis

The cardiac DNA of all the animals at the end of experiment is shown in Figure 6. In control samples (lane 1), the gel electrophoresis DNA presented an intact band. The ISO-treated group revealed laddering of the DNA (lane 2). The combination either with pidogrel (lane 3) or CFPS (lane 4) attenuated the genotoxicity induced by isoproterenol. The obtained results suggest that CFPS treatment protected DNA via inhibiting oxidative stress in myocardial tissue.

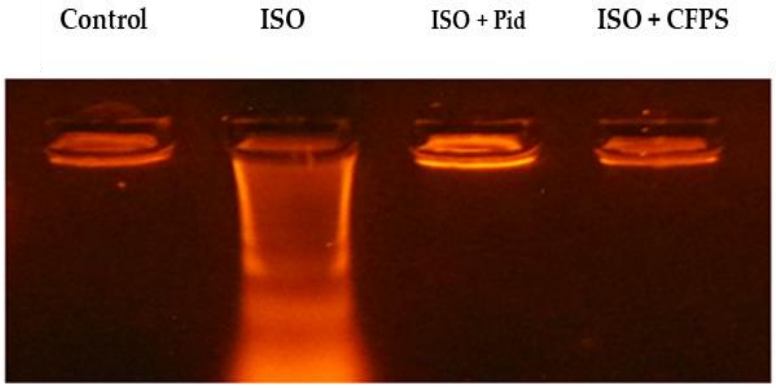

Figure 6. Gel electrophoresis DNA of all treated rats. Lane 1 (control): DNA isolated from the heart tissue of control group; lane 2 (ISO): DNA isolated from group treated with isoproterenol; lane 3 (ISO + Pid): DNA isolated from group precotreated with pidogrel; and lane 4 (ISO + CFPS): DNA isolated from group precotreated with CFPS.

3.3.8. TTC Staining

The TTC method was used to evaluate the myocardial infarction area of all the groups (Figure 7). When compared to the control group, which showed normal red myocardial tissue, ISO treatment led to a large white region (necrotic patches), reflecting a large infarct area. Pretreatment with either CFPS or pidogrel followed by subcutaneous injection of isoproterenol revealed fewer necrotic patches and a marked decrease in the infarction size

compared to the MI group. No differences were observed between the CFPS + ISO and the Pid + ISO groups ($p < 0.05$).

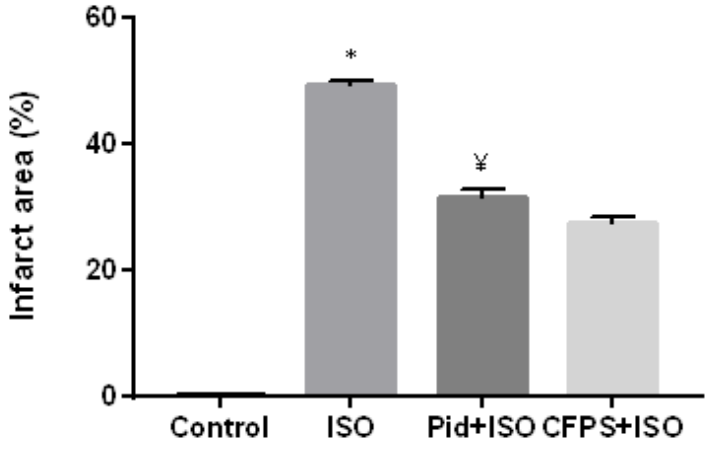

Figure 7. Effect of CFPS on infarct area in control and experimental treated rats as determined by TTC. Values are expressed as mean ± SD of eight rats in each group. * $p < 0.05$: controls vs. ISO. ¥ $p < 0.05$: CFPS + ISO or Pid + ISO vs. ISO.

3.3.9. Histopathological Analysis

The control group showed normal cardiac structure. Nevertheless, the infarcted rats presented separation of myofibrillar, myocardial cells necrosis, and large leucocyte infiltration (Figure 8), which is in harmony with results of previous works [46–51]. However, the ISO-treated group showed myofibrillar distention, necrosis, and inflammatory cell infiltration. The treatment with pidogrel or CFPS (ISO + Pid) and (Iso + CFPS) reduced the edema and the inflammatory cell infiltration in the myocardium. Interestingly, the use of CFPS or pidogrel ameliorated the morphology of cardiac tissue and significantly diminished the necrosis and edema.

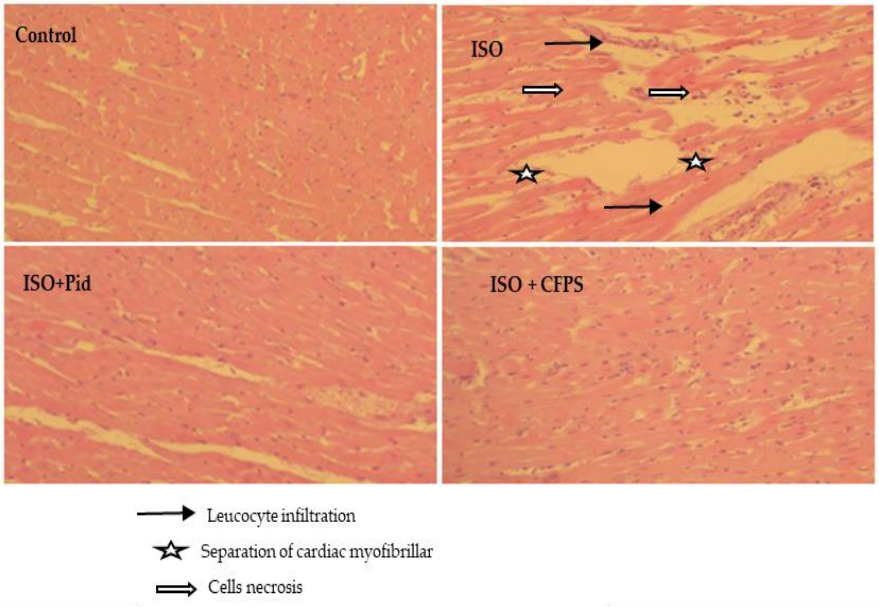

Figure 8. Effect of CFPS precotreatment on histology of myocardial tissue.

4. Discussion

In the current study, 6.5% of crude polysaccharides were successfully extracted from the aerial part of *Clematis flammula* (CFPS) by water extraction and the alcohol precipitation method. The recovery yield of polysaccharides obtained in the present work was similar to

that reported for *Clematis huchouensis* Tamura (6.94%) [22], but higher than that of those extracted from *Camellia oleifera* (1.8%) [52] and pistachio external hull (4.10%) [53]. However, the obtained yield in the current study was lower than that obtained by Fan et al. [54] for acidic polysaccharides from *Citrus grandis*. The observed differences could be due to the effect of various procedures for storing, drying, and extracting samples [55]. The uronic acid content of the polysaccharides was estimated to be 17.81, demonstrating NaCl concentration dependency [55].

As described in the previous section for the FT-IR analysis, the footprint of CFPS showed characteristic bands corresponding to O-H stretching vibrations of both carbohydrates and water [56], stretching and bending vibrations of C-H (CH, CH_2, and CH_3) forms [57], vibrations of carboxylate overlapping with glucoside/glucuronide traces, and stretching of C−C of carbohydrates. The presence of pyran rings in the polysaccharidic structure has been previously confirmed [58,59], as well as β-glycosidic bond deformation and possible α-glycosidic linkages [60].

The result for the monosaccharide content showed remarkable variation as compared to values seen in the literature, which could be due to the extraction/purification methodologies. It is important to bring to attention that, up to now, studies on the purification, characterization, and biological activities of polysaccharides from the genus *Clematis* have been very limited. Other monosaccharides were extracted from *Aconitum* species belonging to the same family of Ranunculaceae [42]. Thus, heteropolysaccharides composed of glucose and arabinose were observed in *Aconitum coreanum* [42]. A water-soluble polysaccharide composed of glucose monomers was isolated from *Aconitum carmichaeli* [61].

The observed cardiac hypertrophy in vivo was a consequence of necrosis of cardiac muscle fibers induced by inflammatory cells following the acute phase of myocardial infarction, as has been reported by Derbali et al. [62]. ISO-treated rats showed significant modifications in the ECG pattern, indicators of myocardial infarction [50]. The toxic effect could be attributed to the lesion of the cell membrane myocardium [63]. In addition, CFPS has restored the change in heart weight. The effect of CFPS was to reduce the edematous space in the heart and preserve the myocardium membrane integrity.

The plasma troponins T as well as CK, CK-MB, and LDH were elevated in ISO-treated rats, which agrees with previous findings [62–64]. The release of these cardiac biomarkers is a result of the death of myocardial cells and/or a change in membrane permeability [65,66]. The present findings reveal that the combination with CFPS diminished the quantity of these parameters in plasma. The ameliorative role of CFPS extract was probably due to the improvement in the cardiac membrane structure, thereby reducing the release of these biomarkers into the circulation. Similarly, Yang et al. [67] showed that a heteropolysaccharide (named CALB-3) extracted from *Fructus aurantii* was able to reduce the level of serum cardiac enzymes and enhance histological damage following myocardial injury in vivo.

The histopathology studies of the cardiac tissue using H&E staining were carried out to further support the biochemical results. The ISO-treated rats presented separation of cardiac myofibrillar, myocardial cells necrosis, and vast inflammatory cell infiltration. The obtained results are in harmony with previous studies [68,69]. An ameliorative state of the morphology of cardiac tissues was detected when using CFPS or pidogrel. The fibrinogen change is an indicator of a myocardial infarction [63,64]. The data of the present findings indicate a high level of plasmatic fibrinogen in the ISO group.

Previous studies have revealed remarkable increases in the level of this glycoprotein in the heart tissue of intoxicated rats, suggesting thrombi residue formation [63,70]. The antithrombotic effect of CFPS extract could be due to the reduction in fibrin polymerization, which minimizes the size of clots [47]. These findings are in harmony with the results previously reported by Han et al. [48], who suggested that water-soluble polysaccharides from *Astragalus membranaceus* were effective against the endothelial dysfunction through their anti-inflammatory effects.

In the current work, the excessive lipid content was a major risk factor for myocardial infarction [71]. The increased level of LDL-C could induce an accumulation of cholesterol in

ISO-treated rats [72]. The elevated triglyceride amount was a result of increased hydrolysis of stored triglycerides via the lipase hormone, as has been proposed previously [63].

The administration of CFPS near normalized the levels of total cholesterol, triglycerides, and LDL cholesterol in the plasma of ISO-induced myocardial-infarcted rats. Various mechanisms can be suggested to explain the attenuation of the lipid profiles. Yang et al. [73] demonstrated that polysaccharide polymers from *Cyclocarya paliurus* exert their anti-hyperlipidemic effect by modulating fatty acid synthesis gene expression. In addition, Ren et al. [74] and Hu et al. [75] suggested that the sulfated polysaccharide from *Enteromorpha prolifera* may ameliorate lipid changes by inhibiting the expression of proteins and/or by modulation of the activities of peroxisome-proliferator-activated receptor (PPARγ and PPARδ).

Moreover, animals treated with CFPS or pidogrel revealed a significant reduction in MDA levels. The reduced levels of MDA might be due to a reactive oxygen species (ROS)-scavenging capacity. These results suggest that CFPS could considerably scavenge ROS generated in the ISO-treated group, as has been proposed by Yang et al. [65] and Rjeibi et al. [26].

These results are supported by DNA fragmentation analysis. The result reveals ISO-induced DNA fragmentation, which is in line with results reported by Liu et al. [76]. The results also show that CFPS precotreatment decreased the alteration in the DNA profile induced by ISO administration. This effect confirmed the powerful antioxidative and ROS-scavenging capacity of this CFPS extract, thereby allowing DNA protection against cellular damage induced by free radicals [77].

5. Conclusions

To our knowledge, this is the first study that targets the partial characterization and some biological properties of polysaccharides from *Clematis flammula*. CFPS revealed protective efficacy against isoproterenol-induced MI. The beneficial role of CFPS included an improved ECG pattern and lipid profile, as well as reduced cardiac dysfunctional markers. The results also show that CFPS reduced the DNA fragmentation and increased the antioxidant enzyme activities together with reducing the lipid peroxidation. These outcomes also highlight the potential use of polysaccharides extracted from *C. flammula* as natural preservatives in the food, cosmetic, and pharmaceutical industries.

Supplementary Materials: The following supporting information can be downloaded at: https://www.mdpi.com/xxx/s1, Figure S1: TIC of the CFPS fraction (A) and MS spectra of the identified residues (B) after the trimethylsilylation step and analyses by GC/MS-EI; Figure S2: Effect of CFPS pre-cotreatment on the ST segment of control and experimental animals; Figure S3: HPLC-SEC/RID profile of CFPS.

Author Contributions: Conceptualization, G.P., I.B. and L.G.; methodology, I.R., G.P., A.F. and I.B.; validation, I.R., G.P. and A.F.; formal analysis, G.P., M.T., P.M., K.M., D.L.C. and A.M.; writing—original draft preparation, I.B., L.G. and G.P.; writing—review and editing, G.P. and S.C.; supervision, G.P., I.R. and S.C. All authors have read and agreed to the published version of the manuscript.

Funding: This research received no external funding.

Institutional Review Board Statement: The study was conducted in accordance with the Declaration of Helsinki and approved by the Ethics Committee for research in animal experimentation of the Faculty of Sciences of GAFSA (Gafsa, Tunisia), approval code FSG-AE-20-23, 12 February 2019.

Informed Consent Statement: Not applicable.

Data Availability Statement: Not applicable.

Acknowledgments: The authors thank Christine Gardarin and Farah Hadjkacem, Université Clermont Auvergne, as well as Christophe Rihouey, Normandie University, UNIROUEN, INSA Rouen, for providing technical support.

Conflicts of Interest: The authors declare no conflict of interest.

References

1. Wang, S.B.; Tian, S.; Yang, F.; Yang, H.G.; Yang, X.Y.; Du, G.H. Cardioprotective effect of salvianolic acid A on isoproterenol-induced myocardial infarction in rats. *Eur. J. Pharmacol.* **2009**, *615*, 125–132. [CrossRef] [PubMed]
2. Radhiga, T.; Rajamanickam, C.; Senthil, S.; Pugalendi, K.V. Effect of ursolic acid on cardiac marker enzymes. lipid profile and macroscopic enzyme mapping assay in isoproterenolinduced myocardial ischemic rats. *Food Chem. Toxicol.* **2012**, *50*, 3971–3977. [CrossRef] [PubMed]
3. Zhou, C.; Cui, Q.; Su, G.; Guo, X.; Liu, X.; Zhang, G. MicroRNA-208b Alleviates post-infarction myocardial fibrosis in a rat model by inhibiting GATA4. *Med. Sci. Monit.* **2016**, *22*, 1808–1816. [CrossRef]
4. Buja, L.M.; Entman, M.L. Modes of Myocardial Cell Injury and Cell Death in Ischemic Heart Disease. *Circulation* **1998**, *98*, 1355–1357. [CrossRef] [PubMed]
5. Reed, G.W.; Rossi, J.E.; Cannon, C.P. Acute myocardial infarction. *Lancet* **2017**, *389*, 197–210. [CrossRef]
6. Rona, G.; Chappel, C.I.; Balazs, T.; Gaudry, R. An infarct-like myocardial lesion and other toxic manifestations produced by isoproterenol in the rat. *Arch. Pathol.* **1959**, *67*, 443–455. Available online: https://cir.nii.ac.jp/crid/1573105974856922496 (accessed on 28 November 2021).
7. de Sànchez, V.C.; Hernández-Muñoz, R.; López-Barrera, F.; Yañez, L.; Vidrio, S.; Suárez, J.; Cota-Garza, M.; Aranda-Fraustro, A.; Cruz, D. Sequential changes of energy metabolism and mitochondrial function in myocardial infarction induced by isoproterenol in rats: A long-term and integrative study. *Can. J. Physiol. Pharmacol.* **1997**, *75*, 1300–1311. [CrossRef]
8. Rona, G. Catecholamine cardiotoxicity. *J. Mol. Cell. Cardiol.* **1985**, *17*, 291–306. [CrossRef]
9. Tasatargil, A.; Kuscu, N.; Dalaklioglu, S.; Adiguzel, C.; Celik-Ozenci, S.; Ozdem, A.; Barutcigil, S.; Ozdem, S. Cardioprotective effect of nesfatin-1 against isoproterenol-induced myocardial infarction in rats: Role of the Akt/GSK-3β pathway. *Peptides* **2017**, *95*, 1–9. [CrossRef]
10. Al-Olayan, E.M.; El-Khadragy, M.F.; Metwally, D.M.; Abdel Moneim, A.E. Protective effects of pomegranate (Punica granatum) juice on testes against carbon tetrachloride intoxication in rats. *BMC Complement. Altern. Med.* **2014**, *14*, 164. [CrossRef]
11. Aune, D.; Giovannucci, E.; Boffetta, P.; Fadnes, L.T.; Keum, N.; Norat, T. Fruit and vegetable intake and the risk of cardiovascular disease, total cancer and all-cause mortality—A systematic review and dose-response meta-analysis of prospective studies. *Int. J. Epidemiol.* **2017**, *46*, 1029–1056. [CrossRef] [PubMed]
12. Deng, X.-Y.; Chen, J.-J.; Li, H.-Y.; Ma, Z.-Q.; Ma, S.-P.; Fu, Q. Cardioprotective effects of timosaponin B II from *Anemarrhenae asphodeloides* Bge on isoproterenol-induced myocardial infarction in rats. *Chem.-Biol. Interactions* **2015**, *240*, 22–28. [CrossRef] [PubMed]
13. Vellosa, J.; Khalil, N.; Formenton, V.; Ximenes, V.; Fonseca, L.; Furlan, M.; Brunetti, I.; Oliveira, O. Antioxidant activity of *Maytenus ilicifolia* root bark. *Fitoterapia* **2006**, *77*, 243–244. [CrossRef] [PubMed]
14. Kumaran, A.; Karunakaran, R.J. Activity-guided isolation and identification of free radical-scavenging components from an aqueous extract of *Coleus aromaticus*. *Food Chem.* **2007**, *100*, 356–361. [CrossRef]
15. Song, M.; Huang, L.; Zhao, G.; Song, Y. Beneficial effects of a polysaccharide from *Salvia miltiorrhiza* on myocardial ischemia–reperfusion injury in rats. *Carbohydr. Polym.* **2013**, *98*, 1631–1636. [CrossRef]
16. Yu, Y.; Shen, M.; Song, Q.; Xie, J. Biological activities and pharmaceutical applications of polysaccharide from natural resources: A review. *Carbohydr. Polym.* **2018**, *183*, 91–101. [CrossRef]
17. Keys, D.J. *Chinese Herbs, Botany, Chemistry and Pharmacodynamics*; Charles E and Tutle Company: Tokyo, Japan, 1985.
18. Gruenwald, J.; Brendler, T.; Jaenicke, C. *PDR for Herbal Medicines*, 2nd ed.; Medical Economics Company: Montvale, NJ, USA, 2000.
19. Chawla, R.; Kumar, S.; Sharma, A. The genus Clematis (Ranunculaceae): Chemical and pharmacological perspectives. *J. Ethnopharmacol.* **2012**, *143*, 116–150. [CrossRef]
20. Saidi, R.; Khanous, L.; Allah, S.K.; Hamdi, B.; Ayadi, A.; Damak, M.; Hammami, H.; Mezghani-Jarraya, R. Antifungal, molluscicidal and larvicidal assessment of anemonin and *Clematis flammula* L. extracts against mollusc *Galba truncatula*, intermediate host of Fasciola hepatica in Tunisia. *Asian Pac. J. Trop. Med.* **2017**, *10*, 967–973. [CrossRef]
21. Atmani, D.; Larrea, M.R.; Sanz, J.R.; Lizcano, L.; Bakkali, F. Antioxidant potential, cytotoxic activity and phenolic content of *Clematis flammula* leaf extracts. *J. Med. Plants Res.* **2011**, *5*, 589–598. [CrossRef]
22. Zhang, Z.; Wang, X.; Zhao, M.; Qian, K. Optimization of polysaccharides extraction from *Clematis huchouensis* Tamura and its antioxidant activity. *Carbohydr. Polym.* **2014**, *111*, 762–767. [CrossRef]
23. Zhu, Y.; Di, S.; Hu, W.; Feng, Y.; Zhou, Q.; Gong, B.; Tang, X.; Liu, J.; Zhang, W.; Xi, M.; et al. A new flavonoid glycoside (APG) isolated from *Clematis tangutica* attenuates myocardial ischemia/reperfusion injury via activating PKCε signaling. *Biochim. Biophys. Acta (BBA)—Mol. Basis Dis.* **2017**, *1863*, 701–711. [CrossRef] [PubMed]
24. Tian, X.R.; Feng, J.T.; Ma, Z.Q.; Xie, N.; Zhang, J.; Zhang, X.; Tang, H.F. Three new glycosides from the whole plant of *Clematis lasiandra* Maxim and their cytotoxicity. *Phytochem. Lett.* **2014**, *10*, 168–172. [CrossRef]
25. Saidi, R.; Ghrab, F.; Kallel, R.; Feki, A.E.; Boudawara, T.; Chesné, C. Tunisian *Clematis flammula* Essential Oil Enhances Wound Healing: GC-MS Analysis. Biochemical and Histological Assessment. *J. Oleo Sci.* **2018**, *67*, 1483–1499. [CrossRef] [PubMed]
26. Rjeibi, I.; Feriani, A.; Hentati, F.; Hfaiedh, N.; Michaud, P.; Pierre, G. Structural characterization of water-soluble polysaccharides from *Nitraria retusa* fruits and their antioxidant and hypolipidemic activities. *Int. J. Biol. Macromol.* **2019**, *129*, 422–432. [CrossRef] [PubMed]

27. Dubois, M.; Gilles, K.A.; Hamilton, J.K.; Rebers, P.; Smith, F. Colorimetric method for determination of sugars and related substances. *Anal. Chem.* **1956**, *28*, 350–356. [CrossRef]
28. Monsigny, M.; Petit, C.; Roche, A.C. Colorimetric determination of neutral sugars by a resorcinol sulfuric acid micromethod. *Anal. Biochem.* **1988**, *175*, 525–530. [CrossRef]
29. Blumenkrantz, N.; Asboe-Hansen, G. New method for quantitative determination of uronic acids. *Anal. Biochem.* **1973**, *54*, 484–489. [CrossRef]
30. Singleton, V.L.; Orthofer, R.; Lamuela-Raventós, R.M. Analysis of total phenols and other oxidation substrates and antioxidants by means of Folin-Ciocalteu reagent. *Methods Enzymol.* **1999**, *299*, 152–178. [CrossRef]
31. Bradford, M. A Rapid and sensitive method for the quantitation of microgram quantities of protein utilizing the principle of protein-dye binding. *Anal. Biochem.* **1976**, *72*, 248–254. [CrossRef]
32. Pierre, G.; Graber, M.; Rafiliposon, B.A.; Dupuy, C.; Orvain, F.; De Crignis, M.; Maugard, T. Biochemical Composition and Changes of Extracellular Polysaccharides (ECPS) Produced during Microphytobenthic Biofilm Development (Marennes-Oléron, France). *Microb. Ecol.* **2011**, *63*, 157–169. [CrossRef]
33. Pierre, G.; Zhao, J.M.; Orvain, F.; Dupuy, C.; Klein, G.L.; Graber, M.; Maugard, T. Seasonal dynamics of extracellular polymeric substances (EPS) in surface sediments of a diatom-dominated intertidal mudflat (Marennes–Oléron, France). *J. Sea Res.* **2014**, *92*, 26–35. [CrossRef]
34. Mnafgui, K.; Khlif, I.; Hajji, R.; Derbali, F.; Kraiem, F.; Ellefi, F.; Gharsallah, N.; Allouche, N. Preventive effects of oleuropein against cardiac remodeling after myocardial infarction in Wistar rat through inhibiting angiotensin-converting enzyme activity. *oxicol. Mech. Methods* **2015**, *25*, 538–546. [CrossRef]
35. Ohkawa, H.; Ohishi, N.; Yagi, K. Assay for lipid peroxides in animal tissues by thiobarbituric acid reaction. *Anal. Biochem.* **1979**, *95*, 351–358. [CrossRef]
36. Chtourou, Y.; Aouey, B.; Kebieche, M.; Fetoui, H. Protective role of naringin against cisplatin induced oxidative stress, inflammatory response and apoptosis in rat striatum via suppressing ROS-mediated NF-κB and P53 signaling pathways. *Chem. Interactions* **2015**, *239*, 76–86. [CrossRef] [PubMed]
37. Sellins, K.S.; Cohen, J.J. Nuclear Changes in the Cytotoxic T Lymphocyte-induced Model of Apoptosis. *Immunol. Rev.* **1995**, *146*, 266. [CrossRef] [PubMed]
38. Khalil, P.N.; Siebeck, M.; Huss, R.; Pollhammer, M.; Khalil, M.N.; Neuhof, C.; Fritz, H. Histochemical assessment of early myocardial infarction using 2,3,5-triphenyltetrazolium chloride in blood-perfused porcine hearts. *J. Pharmacol. Toxicol. Methods* **2006**, *54*, 307–312. [CrossRef]
39. RuiDian, K.; ShunFa, L.; Yi, C.; ChuRong, J.; QiaGuang, S. Analysis of chemical composition of polysaccharides from Poria cocos Wolf and its anti-tumor activity by NMR spectroscopy. *Carbohydr. Polym.* **2010**, *80*, 31–34. [CrossRef]
40. Habibi, Y.; Mahrouz, M.; Marais, M.-F.; Vignon, M.R. An arabinogalactan from the skin of *Opuntia ficus-indica* prickly pear fruits. *Carbohydr. Res.* **2004**, *339*, 1201–1205. [CrossRef]
41. Song, J.; Wu, Y.; Ma, X.; Feng, L.; Wang, Z.; Jiang, G.; Tong, H. Structural characterization and α-glycosidase inhibitory activity of a novel polysaccharide fraction from *Aconitum coreanum*. *Carbohydr. Polym.* **2019**, *230*, 115586. [CrossRef]
42. Kalegowda, P.; Chauhan, A.S.; Urs, S.M.N. *Opuntia dillenii* (Ker-Gawl) Haw cladode mucilage: Physico-chemical, rheological and functional behavior. *Carbohydr. Polym.* **2017**, *157*, 1057–1064. [CrossRef]
43. Bandyopadhyay, S.S.; Navid, M.H.; Ghosh, T.; Schnitzler, P.; Ray, B. Structural features and in vitro antiviral activities of sulfated polysaccharides from Sphacelaria indica. *Phytochemistry* **2011**, *72*, 276–283. [CrossRef] [PubMed]
44. Sengkhamparn, N.; Verhoef, R.; Schols, H.A.; Sajjaanantakul, T.; Voragen, A.G.J. Characterisation of cell wall polysaccharides from okra (*Abelmoschus esculentus* (L.) Moench). *Carbohydr. Polym.* **2009**, *344*, 1824–1832. [CrossRef] [PubMed]
45. Petera, B.; Delattre, C.; Pierre, G.; Wadouachi, A.; Elboutachfaiti, R.; Engel, E.; Poughon, L.; Michaud, P.; Fenoradosoa, T.A. Characterization of arabinogalactan-rich mucilage from *Cereus triangularis* cladodes. *Carbohydr. Polym.* **2015**, *127*, 372–380. [CrossRef] [PubMed]
46. Feriani, A.; Khdhiri, E.; Tir, M.; Elmufti, A.; Tlili, N.; Hajji, R.; Mnafgui, K. (E)-N′-(1-(7-Hydroxy-2-Oxo-2H-Chromen-3-Yl) Ethylidene) benzohydrazide, a novel synthesized coumarin, ameliorates isoproterenol-induced myocardial infarction in rats through attenuating oxidative stress, inflammation, and apoptosis. *Oxid. Med. Cell. Longev.* **2020**, *2020*, 2432918. [CrossRef] [PubMed]
47. Han, R.; Tang, F.; Lu, C.; Xu, J.; Hu, J.; Mei, M.; Wang, H. Protective effects of Astragalus polysaccharides against endothelial dysfunction in hypertrophic rats induced by isoproterenol. *Int. Immunopharmacol.* **2016**, *38*, 306–312. [CrossRef]
48. Prince, P.C.M.; Hemalatha, K.L. A molecular mechanism on the antiapoptotic effects of zingerone in isoproterenol induced myocardial infarcted rats. *Eur. J. Pharmacol.* **2018**, *821*, 105–111. [CrossRef]
49. Mnafgui, K.; Hajji, R.; Derbali, F.; Khlif, I.; Kraiem, F.; Ellefi, H.; Allouche, N.; Gharsallah, N. Protective effect of hydroxytyrosol against cardiac remodeling after isoproterenol-induced myocardial infarction in Rat. *Cardiovasc. Toxicol.* **2016**, *16*, 147–155. [CrossRef]
50. Hamed, M.; Bougatef, H.; Karoud, W.; Krichen, F.; Haddar, A.; Bougatef, A.; Silaa, A. Polysaccharides extracted from pistachio external hull: Characterization, antioxidant activity and potential application on meat as preservative. *Ind. Crop. Prod.* **2020**, *148*, 112315. [CrossRef]

51. Fan, R.; Xie, Y.; Zhu, C.; Qiu, D.; Zeng, J.; Liu, Z. Structural elucidation of an acidic polysaccharide from *Citrus grandis* "Tomentosa" and its anti-proliferative effects on LOVO and SW620 cells. *Int. J. Biol. Macromol.* **2019**, *138*, 511–518. [CrossRef]
52. Hammami, N.; Ben Gara, A.; Bargougui, K.; Ayedi, H.; Ben Abdalleh, F.; Belghith, K. Improved in vitro antioxidant and antimicrobial capacities of polysaccharides isolated from *Salicornia arabica*. *Int. J. Biol. Macromol.* **2018**, *120*, 2123–2130. [CrossRef]
53. Ghanem, M.E.; Han, R.; Classen, B.; Quetin-Leclerq, J.; Mahy, G.; Ruan, C.-J.; Qin, P.; Alfocea, F.P.; Lutts, S. Mucilage and polysaccharides in the halophyte plant species *Kosteletzkya virginica*: Localization and composition in relation to salt stress. *J. Plant Physiol.* **2010**, *167*, 382–392. [CrossRef] [PubMed]
54. Golbargi, F.; Gharibzahedi, S.M.T.; Zoghi, A.; Mohammadi, M.; Hashemifesharaki, R. Microwave-assisted extraction of arabinan-rich pectic polysaccharides from melon peels: Optimization, purification, bioactivity, and techno-functionality. *Carbohydr. Polym.* **2021**, *256*, 117522. [CrossRef]
55. Liu, J.; Zhao, Y.; Wu, Q.; John, A.; Jiang, Y.; Yang, J.; Liu, H.; Yang, B. Structure characterisation of polysaccharides in vegetable "okra" and evaluation of hypoglycemic activity. *Food Chem.* **2018**, *242*, 211–216. [CrossRef]
56. Zhang, S.; Hea, B.; Ge, J.; Li, H.; Luo, X.; Zhang, H.; Li, Y.; Zhai, C.; Liu, P.; Liu, X.; et al. Extraction, chemical analysis of *Angelica sinensis* polysaccharides and antioxidant activity of the polysaccharides in ischemia–reperfusion rats. *Int. J. Biol. Macromol.* **2010**, *47*, 546–550. [CrossRef] [PubMed]
57. Rozi, P.; Abuduwaili, A.; Ma, S.; Bao, X.; Xu, H.; Zhu, J.; Yadikar, N.; Wang, J.; Yang, X.; Yili, A. Isolations, characterizations and bioactivities of polysaccharides from the seeds of three species Glycyrrhiza. *Int. J. Biol. Macromol.* **2020**, *145*, 364–371. [CrossRef]
58. El-Naggar, N.E.; Hussein, M.H.; Shaaban-Dessuuki, S.A.; Dalal, S.R. Production, extraction and characterization of *Chlorella vulgaris* soluble polysaccharides and their applications in AgNPs biosynthesis and biostimulation of plant growth. *Sci. Rep.* **2020**, *10*, 3011. [CrossRef] [PubMed]
59. Zhao, C.; Li, M.; Luo, Y.; Wu, W. Isolation and structural characterization of an immunostimulating polysaccharide from fuzi, *Aconitum carmichaeli*. *Carbohydr. Res.* **2006**, *341*, 485–491. [CrossRef] [PubMed]
60. Derbali, A.; Mnafgui, K.; Affes, M.; Derbali, F.; Hajji, R.; Gharsallah, N.; Allouche, N.; El Feki, A. Cardioprotective effect of linseed oil against isoproterenol-induced myocardial infarction in Wistar rats: A biochemical and electrocardiographic study. *J. Physiol. Biochem.* **2015**, *71*, 281–288. [CrossRef]
61. Ghazouani, L.; Khdhiri, E.; Elmufti, A.; Feriani, A.; Tir, M.; Baaziz, I.; Mnafgui, K. Cardioprotective effects of (E)-4-hydroxy-N′-(1-(3-oxo-3H-benzo[f]chromen-2-yl)ethylidene) benzohydrazide: A newly synthesized coumarin hydrazone against isoproterenol-induced myocardial infarction in a rat model. *Can. J. Physiol. Pharmacol.* **2019**, *97*, 989–998. [CrossRef]
62. Panda, S.; Kar, A.; Ramamurthy, V. Cardioprotective effect of vincristine on isoproterenol-induced myocardial necrosis in rats. *Eur. J. Pharmacol.* **2014**, *723*, 451–458. [CrossRef]
63. Khalil, M.I.; Ahmmed, I.; Ahmed, R.; Tanvir, E.M.; Afroz, R.; Paul, S.; Hua Gan, S.; Alam, N. Amelioration of isoproterenol-induced oxidative damage in rat myocardium by with aniasomnifera leaf extract. *BioMed Res. Int.* **2015**, *2015*, 624159. [CrossRef] [PubMed]
64. Kumar, M.; Kasala, E.R.; Bodduluru, L.N.; Dahiya, V.; Lahkar, M. Baicalein protects isoproterenol induced myocardial ischemic injury in male Wistar rats by mitigating oxidative stress and inflammation. *Inflamm. Res.* **2016**, *65*, 613–622. [CrossRef] [PubMed]
65. Yang, Y. Cardioprotective effects of a Fructus Aurantii polysaccharide in isoproterenol-induced myocardial ischemic rats. *Int. J. Biol. Macromol.* **2020**, *155*, 995–1002. [CrossRef] [PubMed]
66. Shojaie, M.; Pourahmad, M.; Eshraghian, A.; Izadi, H.R.; Naghshvar, F. Fibrinogen as a risk factor for premature myocardial infarction in Iranian patients: A case control study. *Vasc. Health Risk Manag.* **2009**, *5*, 673–676. [PubMed]
67. Machlus, K.R.; Cardenas, J.C.; Church, F.C.; Wolberg, A.S. Causal relationship between hyperfibrinogenemia, thrombosis, and resistance to thrombolysis in mice. *Blood* **2011**, *117*, 4953–4963. [CrossRef]
68. Murugesan, S.; Pandiyan, A.; Saravanakumar, L.; Moodley, K.; Mackraj, I. Protective role of wild garlic on isoproterenol-induced myocardial necrosis in wistar rats. *J. Ethnopharmacol.* **2019**, *237*, 108–115. [CrossRef]
69. Zhang, S.; Li, X. Hypoglycemic activity in vitro of polysaccharides from *Camellia oleifera* Abel, seed cake. *Int. J. Biol. Macromol.* **2018**, *115*, 811–819. [CrossRef]
70. Walton, B.L.; Getz, T.M.; Bergmeier, W.; Lin, F.-C.; de Willige, S.U.; Wolberg, A.S. The fibrinogen γA/γ′ isoform does not promote acute arterial thrombosis in mice. *J. Thromb. Haemost.* **2014**, *12*, 680–689. [CrossRef]
71. Vijayakumar, R.; Nachiappan, V. Cassia auriculata flower extract attenuates hyperlipidemia in male Wistar rats by regulating the hepatic cholesterol metabolism. *Biomed. Pharmacother.* **2017**, *95*, 394–401. [CrossRef]
72. Anandan, R.; Mathew, S.; Sankar, T.V.; Viswanathan, P.G. Protective effect of n-3 polyunsaturated fatty acids concentrate on isoproterenol-induced myocardial infarction in rats. *Prostaglandins Leukot. Essent. Fat. Acids* **2007**, *76*, 153–158. [CrossRef]
73. Yang, Z.; Wang, J.; Li, J.; Xiong, L.; Chen, H.; Liu, X.; Wang, W. Antihyperlipidemic and hepatoprotective activities of polysaccharide fraction from *Cyclocaryapaliurus* in high-fat emulsion-induced hyperlipidaemic mice. *Carbohydr. Polym.* **2018**, *183*, 11–20. [CrossRef] [PubMed]
74. Ren, Z.; Li, J.; Xu, N.; Zhang, J.; Song, X.; Wang, X.; Gao, Z.; Jing, H.; Li, S.; Zhang, C.; et al. Anti-hyperlipidemic and antioxidant effects of alkali-extractable mycelia polysaccharides by *Pleurotus eryngii* var. tuolensis. *Carbohydr. Polym.* **2017**, *175*, 282–292. [CrossRef] [PubMed]
75. Hu, W.B.; Zhao, J.; Chen, H.; Xiong, L.; Wang, W.J. Polysaccharides from *Cyclocaryapaliurus*: Chemical composition and lipid-lowering effect on rats challenged with high-fat diet. *J. Funct. Foods* **2017**, *36*, 262–273. [CrossRef]

76. Liu, D.; Chen, L.; Zhao, J.; Cui, K. Cardioprotection activity and mechanism of Astragalus polysaccharide in vivo and in vitro. *Int. J. Biol. Macromol.* **2018**, *111*, 947–952. [CrossRef]
77. Feriani, A.; Tir, M.; Gómez-Caravaca, A.M.; Contreras, M.D.M.; Talhaoui, N.; Taamalli, A.; Segura-Carretero, A.; Ghazouani, L.; Mufti, A.; Tlili, N.; et al. HPLC-DAD-ESI-QTOF-MS/MS profiling of *Zygophyllum album* roots extract and assessment of its cardioprotective effect against deltamethrin-induced myocardial injuries in rat, by suppression of oxidative stress-related inflammation and apoptosis via NF-κB signaling pathway. *J. Ethnopharmacol.* **2019**, *247*, 112266. [CrossRef]